Available online at www.sciencedirect.com

ScienceDirect

Procedia Engineering 109 (2015) 320 – 326

Procedia Engineering

www.elsevier.com/locate/procedia

XXIII Italian Group of Fracture Meeting, IGFXXIII

Considerations on acoustic emissions in Ti Grade 5 during fatigue test

Claudia Barile, Caterina Casavola*, Giovanni Pappalettera, Carmine Pappalettere

Politecnico di Bari, Dipartimento di Meccanica, Matematica e Management, Viale Japigia 182, 70126 Bari, Italy

Abstract

In this paper the behavior of Ti grade 5 specimens during fatigue tests, subjected to uniaxial sinusoidal load, was studied by using an Acoustic Emission (AE) detection system. A couple of detectors was placed on the sample in order to allow localization of the acoustic source. Slots were preliminary cut into the specimens in order to introduce a region of stress concentration. During the whole test all data characterizing the AE were collected, i.e. number of hits, amplitude of the recorded waveform, longitudinal coordinate of the acoustic source etc. Data were analyzed also applying different kinds of post-processing filters in order to isolate, for example, only events occurring in the higher stress region or having amplitude beyond a given selected levels. The system proved itself to have a good capability to localize the crack while, properly filtered cumulative graph of hits, display features strictly connected with the nucleation, and propagation of the cracks. Finally amplitude analysis of the recorded signal shows that two main bands of amplitude were recorded during the test.

Peer-review under responsibility of the Gruppo Italiano Frattura (IGF)

Keywords: Acoustic Emission; Fatigue; Titanium grade 5, Crack Propagation

1. Introduction

Titanium and Titanium alloys are materials of great interest in engineering field because of their excellent mechanical properties. They have high resistance to corrosion and fatigue, good mechanical properties at high temperatures, low density and, at the same time, a very good biocompatibility. Aircraft industry, in particular, appears very interested in a wider adoption of this material which would allow to reduce the total mass of the airplane by reducing, as a consequence, the fuel consumption and the greenhouse emissions [1]. Due to the relevance of the matter

* Corresponding author. Tel.: +39-080-5962787; fax: +39-080-5962777.
E-mail address: katia.casavola@poliba.it

Peer-review under responsibility of the Gruppo Italiano Frattura (IGF)
doi:10.1016/j.proeng.2015.06.239

a great number of studies have been carried on fatigue characterization of Ti alloy [2-5] also to take into account the effects of surface treatments [6], the influence of plastic deformations [7] as well as the presence of residual stresses [8]. Effects on fatigue performances have also been evaluated for different methods of production of complex parts like laser or hybrid welding [9,10], selective electron beam melting [11], friction stir welding [12] or selective laser melting [13]. More insight can be achieved by applying innovative monitoring techniques to specimen subjected to fatigue loading, in this paper, in particular, the acoustic emission (AE) was adopted in order to get some more clues about what is happening, in real time, inside the sample under testing. One of the main advantages of this technique is, in fact, that it allows continuous monitoring of structures without any necessity to stop the test [14]. The method is based on the detection of the stress wave originated by an active defect inside the material [15]. The acoustic wave can be detected by using piezoelectric sensors properly placed on the surface of the specimen under analysis and it has been successfully applied to many different situation as for example the monitoring of the motion of dislocations during local annealing treatments [16-19] or the analysis of the crack propagation in aluminum samples [20] and in steel [21]. Titanium alloy have been studied by AE in [22-23] where however no consideration about acoustic source localization and choice of amplitude and spatial filter is present. In this paper a couple of piezoelectric acoustic sensors have been placed on a sample subjected to sinusoidal fatigue load, this allow linear localization along the length of the sample of the acoustic source, furthermore different features of acquired acoustic signal were detected as for examples, amplitude, hits and so on and they were compared in different areas in the tested specimen.

Nomenclature

A	Cross section of the samples
l	Length of the samples
r	Radius of the slots
k_t	Stress Concentration Factor
R	Loading Ratio
F	Applied Load
f	Loading Frequency
f_a	Acquisition Frequency
d_s	Distance between the sensors
V_{th}	Threshold Voltage
v	speed of the acoustic wave
d_{1y}	Longitudinal distance of the acoustic event from the sensor 1
d_{2y}	Longitudinal distance of the acoustic event from the sensor 2
T_1	Arrival time of the acoustic wave on the sensor 1
T_2	Arrival time of the acoustic wave on the sensor 2
N	Number of cycles
Ñ	Normalized number of cycles
ε_A	Measured strain amplitude

2. Materials and Methods

Seven Titanium grade 5 samples were tested (Fig. 1). The samples had a rectangular cross section A=40x4 mm^2 and a length l=200 mm. Two slots were laser cut in the sample in order to introduce a stress concentration area that will allow to define the region of crack nucleation and propagation. In such a way it will be possible to test the effectiveness of the AE technique in localize the acoustic emission source. The radius of the slot was r=5 mm and the corresponding stress concentration factor was k_t=3. Fatigue tests were performed, under sinusoidal load, by a Instron servo-hydraulic machine equipped with a 100 kN loading cell. Three different levels of loadings were tested, respectively ± 11kN, ± 15 kN, ± 18 kN with a load ratio R=-1and a load frequency f=3 Hz. Two strain gages were placed next to the slots (Fig.2) and the System 5000 acquisition system was used to acquire their signals. The

acquisition frequency was set to f_a=10 Hz. Two piezoelectric Pico sensors [24] were placed in the upper and in the lower part of the sample symmetrically with respect to the median axis of the sample (Fig.2).

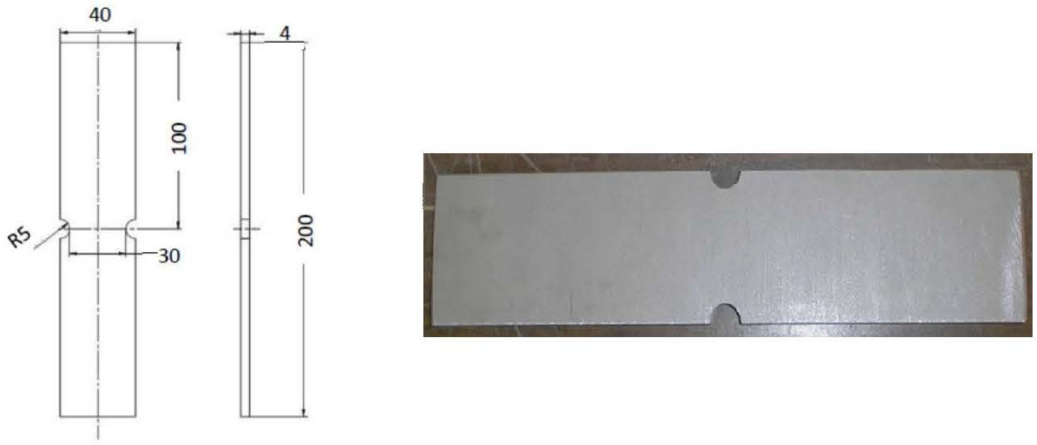

Fig. 1(a) geometry and dimension of the specimens; (b) picture of the specimen.

These sensors have dimensions 5x4 mm and a sensitivity range 200÷750 kHz. Coupling of the sensor with the metal was done through siliconic grease and properly checked by Hsu-Nielsen test.

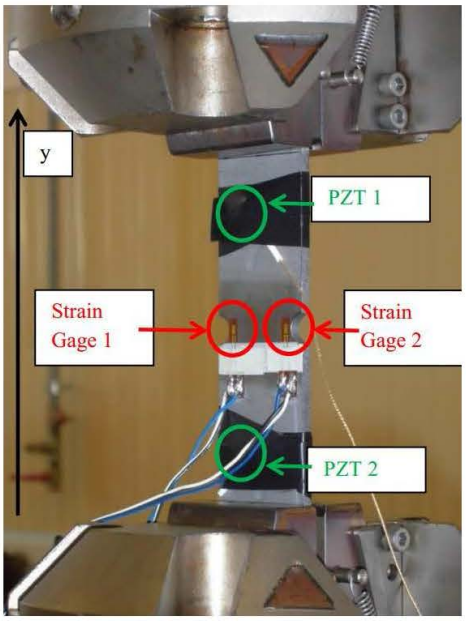

Fig. 2 Picture of the set-up with the indication of the position of the acoustic piezoelectric sensor and the strain gages.

The distance between the two sensors was d_s= 80 mm. The output signals from the PZT sensor were sent to a pre-amplifier modulus having a gain set to 40 dB and, successively, to the acquisition board. Preliminary operations allowed to determine the sound speed for the tested material i.e. v=5500 m/s and the proper threshold value for the AE system. This last parameter was set to V_{th}= 45 dB which was found to be a good compromise between the necessity

to filter noise as best as possible and, at the same time, to maintain a good sensitivity for detection of relevant events. Once that v and d_s are known it is possible to perform linear localization of the AE source by solving the following equation:

$$\left|d_{1y}-d_{2y}\right|=v\cdot\left|T_1-T_2\right| \quad (1)$$

By knowing that:

$$d_s=d_{1y}+d_{2y} \quad (2)$$

Finally recorded AE signal were collected and analyzed by the PAC software which also allow the possibility to perform some post-processing operation like spatial and amplitude filtering.

3. Results and Discussions

In Fig.3 the ε_a vs N graph is reported on a Log-Log diagram. The strain amplitude reported is that measured by one of the strain gages attached on the samples.
The arrows indicate that two of the tested samples were not broken during the test that in both cases was stopped at about five millions of cycles. The trend is quite well fitted by a power law according to the relationship $\varepsilon_a=5178.9\cdot N^{-0.147}$ the trend is shallow as stated in [25]. The exponent b=-0.147 found for the power law appears to be consistent with other similar measurements like those reported in [26] where an exponent b=-0.104 was found for Ti grade 5.

In Fig.4 the slope of the $F_{vs}\varepsilon$ is plotted as a function of the normalized number of cycles that is to say the current number of cycles divided by the number of cycles to rupture. Data are referred to the two strain gages applied on the specimen number 4 tested at F=±15 kN, however similar behavior have been observed for all the tested specimens.

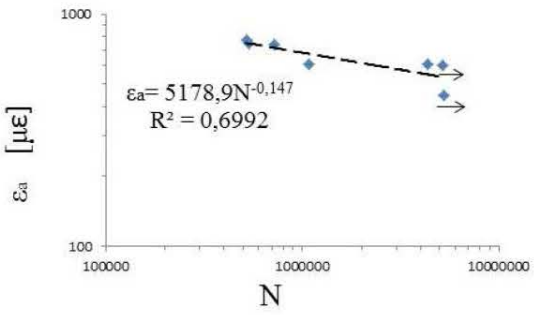

Fig. 3. ε_a vs N curve – arrows are referred to samples which were not broken during the test.

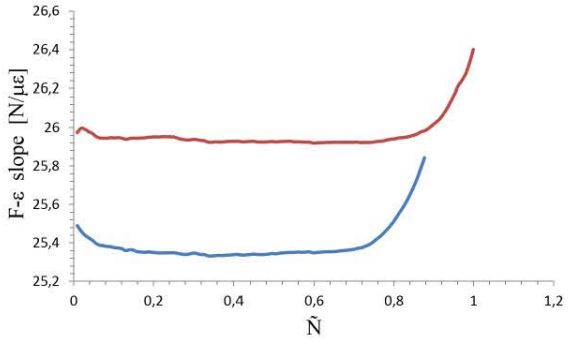

Fig. 4 Slope of the F-ε curve vs Ñ. Plot was obtained for specimen #4 tested at ±15kN.

Plot in Fig.4 shows that due to the propagation of the fatigue crack a sudden increase of the slope appears as a consequence of the reduction of the stiffness of the specimen. This behavior is anticipated by the strain gage nearest to the crack initiation site, whose date are described by the blue line, and where difference in slope are observable at about 75 % of the total life of the sample. Similar behavior is found also on the strain gages placed on the opposite site with respect to the crack initiation area but change in slope are observed later at about 88 % of the total life.

In Fig.5 the cumulate number of counts recorded by one of the two piezoelectric sensors is presented for the specimen numbered 4 and 5.

It can be observed that in both cases there is an initial stage with a more rapid increment of the cumulative number of counts followed by a stabilization of the number of counts. These two stages are commonly observed in AE testing however data does not display the final rapid increment connected with the final stage of crack propagation as it is observed, for example, in [22] and in [27]. A possible explanation for that can be that a great number of events occurs in that stage in the whole sample and this can mask this features. If a high-pass amplitude is applied to data with a threshold of 60 dB the curve appears as it is shown in Fig.6.

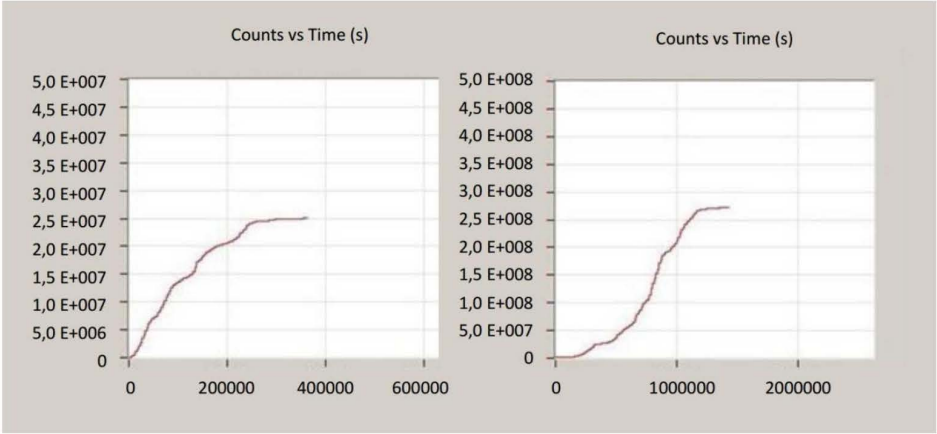

Fig. 5 Cumulative behaviour of the number of counts vs time (left) specimen 4 (right) specimen 5.

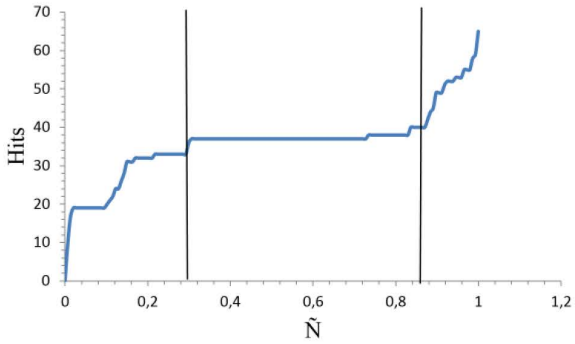

Fig. 6 Hits vs Normalized number of cycles. Number of Hits has been filtered by a high-pass amplitude filter. Data are referred to the specimen number 7.

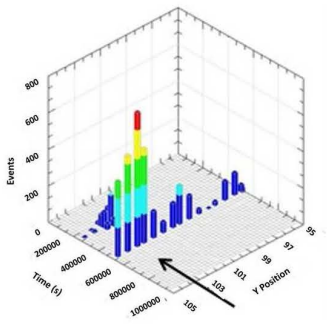

Fig. 7 Events vs Time vs Y position. The area displayed is the region where the maximum density of events was observed. Data are referred to specimen.

It can be observed that, at about 83% of the total life a rapid increment of the slope appears that can be strictly connected with the final stage of the crack propagation. Similar behavior are observed for all the specimen that were broken during the measurements.

Finally in Fig.7 is displayed the portion of the sample where the highest density of high amplitude events are found. The arrows indicate the position of the center of the slots which corresponds to longitudinal coordinate of the crack path. As it can be observed the area is centered about the slots position, this confirms that the high amplitude events are connected to the crack propagation phenomenon and at the same time shows the capability to precisely localize the crack position along the sample by the AE technique.

4. Conclusions

In this paper AE technique was used to monitor defects activity in Ti grade 5 sample subjected to sinusoidal fatigue loading. It was observed that a quite consistent acoustic emission occurs during the whole test. If the cumulative number of counts or hits is properly analyzed in order to isolate higher amplitude events three different stages in crack evolution can be distinguished. In the first stage activity stays high as a consequence of crack initiation. In the second stage the activity is lowered down until approaching the stage next to the unstable crack propagation where the slope of the cumulative number of counts greatly increase until the rupture of the specimen. The onset of this stage approximately corresponds to the increase of the F-ε slope as obtained from the strain gage next to the crack initiation site. With respect to the extensimetric technique, however, AE emission doesn't require pre-knowledge of the crack initiation site because. Finally, provided the correct value of the sound speed in the given material is known, the AE technique proved itself to be efficient in detect the longitudinal position of the crack during all the performed tests.

References

[1] C. Casavola, L. Lamberti, C. Pappalettere, F. Tattoli, A comprehensive numerical stress - Strain analysis of laser beam butt-welded titanium compared with austenitic steel joints, J Strain Anal Eng, 45 (2010) 535-554.
[2] C. Casavola, F. Tattoli, C. Pappalettere, Static and fatigue characterization of titanium alloy welded joints, Conf Proc Sem, 3 (2007) 1400-1411.
[3] C. Casavola, C. Pappalettere, Discussion on local approaches for the fatigue design of welded joints, Int J Fatigue, 31 (2009) 41-49.
[4] C. Casavola, C.Pappalettere, F.Tattoli, Experimental and numerical study of static and fatigue properties of titanium alloy welded joints, Mech Mat, 41 (2009) 231-243.
[5] C. Casavola, R. Nobile, C. Pappalettere, A local strain method for the evaluation of welded joints fatigue resistance: The case of thin main-plates thickness, Fatigue Eng Mater, 28 (2005) 759-767.
[6] R.Sonntag, J. Reinders, J. Gibmeier, J.P. Kretzer, Fatigue performance of medical Ti6Al4V alloy after mechanical surface treatmens, PLoS One, 10 (2015).
[7] V.A. Zhukov, Influence of plastic deformation on fatigue of titanium alloys, Conf Mese, 22 (2015) 137-141.
[8] K. Moussaoui, M. Mousseigne, J. Senatore, R. Chieragatti, The effect of roughness and residual stresses on fatigue life time of an alloy of titanium, Int J Adv Manuf Technol, 78 (2015) 557-563.
[9] C. Casavola, C. Pappalettere, G. Pluvinage, Fatigue resistance of titanium laser and hybrid welded joints, Mater Des, 32 (2011) 3127-3135.
[10] C. Casavola, C. Pappalettere, F. Tursi, Residual stress on Ti6Al4V hybrid and laser welded joints, Conf Proc Sem, 8 (2011) 111-118.
[11] S. Tammas-Williams, H. Zhao, F.Léonard, F. Derguti, I. Todd, P.B. Prangnell, XCT analysis of the influence of melt strategies on defect population in Ti-6Al-4V components manufactured by Selective Electron Beam Melting, Mater Charact, 102 (2015) 47-61.
[12] P. Edwards, M. Ramulu, Fatigue performance of Friction Stir Welded Ti-6Al-4V subjected to various post weld heat treatment temperatures, Int J Fatigue, 75 (2015) 19-27.
[13] W. Xu, S. Suna, J. Elambasseril, Q. Liu, M. Brandt, M. Quian, Ti-6Al-4V Additively Manufactured by Selective Laser Melting with Superior Mechanical Properties, JOM, 67 (2015) 668-673.
[14] R.Geng, Modern acoustic emission technique and its application in aviation industry, Ultrasonics, 44 (2006) e1025-e1029.
[15] T.M. Roberts, M. Talebzadeh, Acoustic emission monitoring of fatigue crack propagation, J Constr Steel Res, 59 (2003) 695-712.
[16] C. Barile, C. Casavola, G. Pappalettera, C. Pappalettere, Feasibility of Local Stress Relaxation by Laser Annealing and X-Ray Measurement, Strain, 49 (2013) 393-398.
[17] C. Barile, C. Casavola, G. Pappalettera, C. Pappalettere, Preliminary Analysis for a New Approach to Relieve Residual Stresses by Laser Heating, Conf Proc 11th IMEKO TC15 YSESM, 2012, pp. 77-82.
[18] C. Barile, C. Casavola, G. Pappalettera, C. Pappalettere, Acoustic emission analysis of aluminum specimen subjected to laser annealing Conf Proc SEM, 8 (2014) 309-315..
[19] C. Barile, C. Casavola, G. Pappalettera, C. Pappalettere, Discussion on the thermal field produced by laser annealing for the residual stress relaxation, Conf. Proc NT2F13, 2013, pp. 22-30.
[20] C. Barile, C. Casavola, G. Pappalettera, C. Pappalettere, Hybrid thermography and acoustic emission testing of fatigue crack propagation in Aluminum Samples, Conf Proc Sem, 66 (5) (2015) 247-252.
[21] N. Nemati, B. Metrovich, A. Nanni, Acoustic emission assesment of through-thickness fatigue crack growth in steel members, Adv Struct Eng, 16 (2015) 269-282.
[22] F. Vlasic, L. Nohal, P. Mazal, P. Liskutin, Study of high-cycle fatigue behaviour of titanium alloy using acoustic emission method, Conf Proc Metal, 2014, pp.1423-1430.
[23] X. Wu, R. Botten, D. Hu, M.H. Loretto, Cracking of TiAl-based alloys and the effect of cracking on fatigue life, Int J Mater Prof Tec, 1 (2001) 269-274.
[24] www.mistrasgroup.com.
[25] N.E. Dowling, Mechanical Beahavior of Materials, second ed., Prentice Hall, Upper Saddle River, 1998.
[26] F.A. Conle, R.W. Landgraf, F.D. Richards, Materials Data Book: Monotonic and Cyclic Properties of Engineering Materials, Ford Moto Co, Dearborn, 1984.

[27] Z.Han, H. Luo, J.Cao, H.Wang, Acoustic emission during fatigue crack propagation in a micro-alloyed steel and welds, Mat Sci Eng A-Struct, 528 (2011) 7751-7756.